

## QM/MM Study of the Role of the Solvent in the Formation of the Charge Separated Excited State in 9,9'-Bianthryl

Ferdinand C. Grozema,<sup>\*,†</sup> Marcel Swart,<sup>‡</sup> Robert W. J. Zijlstra,<sup>‡</sup> Jacob J. Piet,<sup>†</sup>  
Laurens D. A. Siebbeles,<sup>†</sup> and Piet Th. van Duijnen<sup>§</sup>

*Contribution from the DelftChemTech, Section Opto-Electronic Materials, Delft University of Technology, Mekelweg 15, 2629 JB Delft, The Netherlands, Theoretische Chemie, Vrije Universiteit Amsterdam, De Boelelaan 1083, 1081 HV Amsterdam, The Netherlands, and Theoretical Chemistry, Materials Science Center, University of Groningen, Nijenborgh 4, 9747 AG Groningen, The Netherlands*

Received March 18, 2005; E-mail: grozema@tnw.tudelft.nl

**Abstract:** In this paper the role of the solvent in the formation of the charge-separated excited state of 9,9'-bianthryl (BA) is examined by means of mixed molecular mechanical/quantum mechanical (QM/MM) calculations. It is shown that in weakly polar solvents a relaxed excited state is formed with an interunit angle that is significantly smaller than 90°. This relaxed excited state has a considerable dipole moment even in weakly polar solvents; for benzene and dioxane dipole moments of ca. 6 D were calculated, which is close to experimental data. These dipoles are induced by the solvent in the highly polarizable relaxed excited state of BA, and the dipole relaxation time is governed by solvent reorganizations. In polar solvent the charge separation is driven to completion by the stronger dipoles in the solvent and a fully charged separated excited state is formed with an interunit angle of 90°.

### I. Introduction

9,9'-Bianthryl (BA) (Figure 1) is one of the classic examples of symmetric molecules in which the (electronic) symmetry is broken on photoexcitation. In 1968 it was shown by Schneider and Lippert that the fluorescence of bianthryl (BA) exhibits a pronounced bathochromic shift in polar solvents.<sup>1,2</sup> This is indicative of a highly dipolar relaxed S1 state. From the dependence of the fluorescence energy on solvent polarity, the absolute value of the dipole moment of the relaxed S1 state was determined to be ca. 20 D, a value which has been reproduced in several subsequent studies.<sup>3–6</sup> Most of the recent work has been focused on the elucidation of the precise mechanism and dynamics by which the initially formed non-dipolar excited state is transformed into a highly dipolar charge transfer state, in which a full electronic charge is transferred from one anthryl moiety to the other.

In the ground state the two anthracene groups are perpendicular to each other so that they are electronically decoupled. Electronic excitation of bianthryl initially leads to the formation of a nondipolar excited state, usually called the “locally excited

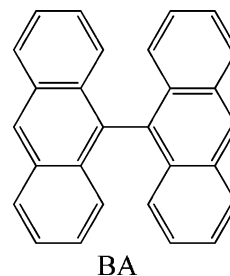


**Figure 1.** Molecular structure of bianthryl (BA).

state” (LE). The absorption spectrum of BA is very similar to that of anthracene and shows virtually no dependence on the solvent polarity, which indicates that the vertically excited state is nonpolar. In polar solvents the observations are quite different. It is well documented that in such solvents a charge-separated excited state is formed which is stabilized by electrostatic interactions with the solvent.<sup>3–5</sup> These observations are in fact analogous to those for so-called twisted intramolecular charge transfer states (TICT) for molecules such as dimethylaminobenzonitrile.<sup>7</sup>

Relaxation of the geometry in nonpolar solvents leads to a smaller angle between the anthryl units. It was shown by Wortmann et al. that the temperature-dependent fluorescence spectra in alkane solvents and benzene can be explained in terms of a neutral excitonic state with a potential energy surface with two minima ca. 62° and 118°. <sup>8,9</sup> Although the emission from

<sup>†</sup> Delft University of Technology.

<sup>‡</sup> Vrije Universiteit Amsterdam.

<sup>§</sup> University of Groningen.

- (1) Schneider, F.; Lippert, E. *Ber. Bunsen-Ges. Phys. Chem.* **1970**, *74*, 624–630.
- (2) Schneider, F.; Lippert, E. *Ber. Bunsen-Ges. Phys. Chem.* **1968**, *72*, 1154–1160.
- (3) Zander, M.; Rettig, W. *Chem. Phys. Lett.* **1984**, *110*, 602–610.
- (4) Müller, J. G.; Heinze, J. *Chem. Phys.* **1991**, *157*, 231–242.
- (5) Fritz, R.; Rettig, W.; Nishiyama, K.; Okada, T.; Müller, U.; Müllen, K. *J. Phys. Chem. A* **1997**, *101*, 2796–2802.
- (6) Nishiyama, K.; Honda, T.; Reis, H.; Müller, U.; Müllen, K.; Baumann, W.; Okada, T. *J. Phys. Chem. A* **1998**, *102*, 2934–2943.
- (7) Grabowski, Z. R.; Rotkiewicz, K.; Rettig, W. *Chem. Rev.* **2003**, *103*, 3899–4031.
- (8) Wortmann, R.; Elich, K.; Lebus, S.; Liptay, W. *J. Chem. Phys.* **1991**, *95*, 6371–6381.

this neutral excitonic state shows almost no dependence on the solvent polarity it was clearly demonstrated by time-resolved microwave conductivity (TRMC)<sup>10–12</sup> and electro-optical emission<sup>13</sup> measurements that the relaxed  $S_1$  state has an appreciable dipole moment, even in saturated hydrocarbon solvents. From TRMC measurements dipole moments between 5 and 8 D were obtained for nonpolar and weakly polar solvents.

A possible explanation for these results is to assume an equilibrium between the neutral excitonic state and a charge-separated state.<sup>4,5,14–16</sup> Such an equilibrium requires that a certain fraction of the BA excited states is in the fully charge-separated state. The equilibrium fraction of excited BA molecules in the charge transfer (CT) state,  $F(CT)$ , has been estimated to be 0.35, 0.70, and 0.74 for BA in *n*-hexane, benzene, and dioxane, respectively, by Barbara et al.<sup>15</sup> and Schütz et al.<sup>16</sup> on the basis of an analysis of fluorescence spectra using an equilibrium model. Such large fractions of charge-separated excited states should, however, give rise to features in transient optical absorption spectra indicating the presence of radical cations or anions of anthracene. Such features have been observed in polar solvents such as acetonitrile and butyronitrile,<sup>5,6,17</sup> but not in weakly polar solvents. Moreover, if the excited-state dipole moments from TRMC measurements are used together with the values for  $F(CT)$  listed above to calculate the dipole moment of the CT state, a value of ca. 8.5 D is obtained which is less than half of the dipole moment for the CT obtained from solvatochromic measurements (20D).<sup>12</sup> Clearly, a simplified two-state equilibrium model is not sufficient to explain all experimental results.

Another interesting aspect of the TRMC measurements is the dipole relaxation time, i.e., the randomization of the net dipole moment, which was found to be on the order of 10 ps for BA in weakly polar solvents. This relaxation time is too short to be explained by rotational diffusion of BA (~200 ps) and therefore was attributed to intramolecular dipole reversal with the time-scale possibly governed by the solvent relaxation time.<sup>11,12</sup>

Quantum chemical calculations can give valuable insight in photophysical processes, since direct information is obtained on the energetics and electronic properties of excited states. Some theoretical work has been done for the photophysics of BA, starting already with Pariser–Pople–Parr-type calculations by Schneider and Lippert.<sup>1</sup> Ab initio molecular orbital calculations were performed by Scholes et al.<sup>18</sup> for solvent-free BA. Grabner et al.<sup>19</sup> have performed semiempirical calculations in which the solvent was modeled by a dielectric continuum.

Although both the latter papers give valuable information on the photophysics of BA, the absence of an explicit treatment of the solvent does not allow any conclusions on the role of the solvent in the excited-state symmetry breaking.

This paper describes, for the first time, a theoretical study of excited state symmetry breaking in which the asymmetric fluctuations in the solvent shell are explicitly accounted for. Semiempirical calculations based on the INDO/s Hamiltonian are presented for BA in which the solvent is included using a hybrid quantum mechanical/molecular mechanical method. The absorption and emission spectra (for the relaxed  $S_1$  state and the CT state) of BA were calculated in several solvents, and the solvent dependence was found to be in good agreement with experimental data. It is shown also that in weakly polar solvents such as benzene and dioxane considerable dipole moments can be induced in the relaxed excited state in BA, without causing an appreciable solvent effect on the emission energy. The direction of the induced dipole moment was found to change on the time scale of molecular reorientations in the solvent, comparable to the dipole relaxation times obtained from TRMC experiments. The presence of a considerable local electric field in weakly polar and nonpolar solvents is of particular importance for the understanding of the role of the solvent in the formation of charge-separated excited states in general, not just for BA itself. Asymmetric solvent shells in weakly polar and nonpolar solvents provide a symmetry breaking mechanism that is at least equally important as intramolecular “vibrational” symmetry breaking.

## II. Computational Methods

**Direct Reaction Field Model.** All quantum chemical calculations discussed in this work were performed in the framework of the (semiempirical) intermediate neglect of differential overlap (INDO) approximation. Calculations on the BA molecules were performed using the spectroscopic parametrization of the INDO Hamiltonian (INDO/s) developed by Zerner and co-workers.<sup>20–23</sup> The optical absorption spectra and electronic properties of the excited states of interest were obtained by configuration interaction (CI) calculations using the Hartree–Fock INDO/s reference wave function.

The inclusion of solvent effects in quantum chemical calculations can be accomplished in several ways. The most widespread method is by employing dielectric continuum methods in which the solute is placed in a cavity in a dielectric continuum representing the surrounding solvent.<sup>24</sup> Although this is very efficient computationally, it is not always sufficient to treat the effect of the solvent in such an approximate way, especially in cases where the specific structure of the first few solvent shells is of interest. Such situations can arise when one or more solvent models interact in a very specific way with the solute.<sup>25</sup> Moreover, a general property of dielectric continuum models is that the surrounding solvent always reflects the symmetry of the solute. In the present work, where the interest is in the role of the solvent as a symmetry-breaking medium, such a continuum model is clearly not sufficient. Therefore a discrete solvent model, the Direct Reaction Field model, in which the structure of the solvent shells is explicitly accounted for, was employed for the present work.

- (9) Wortmann, R.; Lebus, S.; Elich, K.; Assar, S.; Detzer, N.; Liptay, W. *Chem. Phys. Lett.* **1992**, *198*, 220–228.
- (10) Visser, R.-J.; Weisenborn, P. C. M.; van Kan, P. J. M.; Huizer, B. H.; Varma, C. A. G. O.; Warman, J. M.; de Haas, M. P. *J. Chem. Soc., Faraday Trans. 2* **1985**, *81*, 689–704.
- (11) Toublanc, D. B.; Fessenden, R. W.; Hitachi, A. *J. Phys. Chem.* **1989**, *93*, 2893–2896.
- (12) Piet, J. J.; Schuddeboom, W.; Wegewijs, B. R.; Grozema, F. C.; Warman, J. M. *J. Am. Chem. Soc.* **2001**, *123*, 5337–5347.
- (13) Baumann, W.; Spohr, E.; Bischof, H.; Liptay, W. *J. Luminesc.* **1987**, *37*, 227–233.
- (14) Rettig, W.; Zander, M. *Ber. Bunsen-Ges. Phys. Chem.* **1983**, *87*, 1143–1149.
- (15) Kang, T. J.; Kahlow, M. A.; Giser, D.; Swallen, S.; Nagarajan, V.; Jarzeba, W.; Barbara, P. F. *J. Phys. Chem.* **1988**, *92*, 6800–6807.
- (16) Schütz, M.; Schmidt, R. *J. Phys. Chem.* **1996**, *100*, 2012–2018.
- (17) Nishiyama, K.; Honda, T.; Okada, T. *Acta Phys. Pol., A* **1998**, *94*, 847–856.
- (18) Scholes, G. D.; Fournier, T.; Parker, A. W.; Philips, D. *J. Chem. Phys.* **1999**, *111*, 5999–6010.
- (19) Grabner, G.; Rechthaler, K.; Köhler, G. *J. Phys. Chem. A* **1998**, *102*, 689–696.

- (20) Bacon, A. D.; Zerner, M. C. *Theor. Chim. Acta* **1979**, *53*, 21–54.
- (21) Ridley, J.; Zerner, M. C. *Theor. Chim. Acta* **1973**, *32*, 111–134.
- (22) Zerner, M. C. Semiempirical molecular orbital methods. In *Reviews in Computational Chemistry*; Boyd, L., Ed.; VCH: New York, 1991; Vol. 2, pp 313–366.
- (23) Zerner, M. C.; Loew, G. H.; Kirchner, R. F.; Mueller-Westerhoff, U. T. *J. Am. Chem. Soc.* **1980**, *102*, 589–599.
- (24) Tomasi, J.; Persico, M. *Chem. Rev.* **1994**, *94*, 2027–2094.
- (25) Karelson, M.; Zerner, M. C. *J. Am. Chem. Soc.* **1990**, *112*, 9405–9406.

The Direct Reaction Field (DRF) model<sup>26–28</sup> is a hybrid quantum mechanical/molecular mechanical model (QM/MM) in which a quantum chemical description of the molecule(s) of interest (the solute) is combined with a classical mechanical description of the surroundings (the solvent). The DRF model has been successfully employed in studies of the solvent effects on electronic absorption spectra,<sup>29,30</sup> response properties in the condensed phase,<sup>31,32</sup> and studies of solvent-induced symmetry breaking in the excited states of twisted ethylene.<sup>33</sup> Recently, the DRF code has been extended so that it can be used in configuration interaction calculations using the INDO/s method. The general features of the DRF model and its actual implementation have been described in detail on several occasions.<sup>28,32,34</sup> Therefore, only some of the features relevant for the present work are discussed here.

In the DRF model the classically treated solvent molecules are represented by sets of point charges (one on each atom), polarizabilities (either atomic polarizabilities or group polarizabilities for an entire molecule), and repulsion radii. The quantum system is described by a standard quantum chemical method, either single determinant wave functions, such as restricted or unrestricted Hartree–Fock wave functions, or multideterminant configuration interaction wave functions but also by density functional theory.<sup>35</sup> The total energy of the mixed QM/MM system is given by

$$\Delta U^{\text{discr}} = \Delta U^{\text{QM}} + \Delta U^{\text{MM}} + \Delta U^{\text{QM/MM}} \quad (1)$$

In eq 1  $\Delta U^{\text{QM}}$  is the expectation value of the vacuum Hamiltonian of the quantum system over the nonvacuum wave function.  $\Delta U^{\text{MM}}$  is the total energy of the classical system which is a sum of four contributions: the electrostatic interaction (due to the point charges), the induction interaction (due to interaction between point charges and polarizabilities), the van der Waals or dispersion interaction (evaluated by the Slater–Kirkwood relation<sup>36</sup> using the atomic polarizabilities), and the short-range repulsion interaction (evaluated using the repulsion radii).  $\Delta U^{\text{QM/MM}}$  represents the interaction between the quantum system and its classical surroundings, which is given by

$$\begin{aligned} \Delta U^{\text{QM/MM}} = & \sum_{A,i,j} q_i^A v_{ij} Z_j + e \sum_{A,i} q_i^A \langle v \rangle_i \\ & + \sum_{A,i,j,r,s} q_i^A f_{ir} A_{rs} f_{sj} Z_j + e \sum_{A,k,j,r,s} q_j^A f_{jr} A_{rs} \langle f(s;k) \rangle \\ & + \frac{1}{2} \sum_{i,j,r,s} Z_i f_{ir} A_{rs} f_{sj} Z_j + e \sum_{i,k,r,s} Z_i f_{ir} A_{rs} \langle f(s;k) \rangle \\ & + \frac{\gamma}{2} e^2 \sum_{krs} \langle f(k;r) A_{rs} f(s;k) \rangle \\ & + \frac{1}{2} e^2 \sum_{k,l,r,s} \langle f(k;r) A_{rs} \left( 1 - \frac{\gamma}{2} P_{12} \right) \langle f(s;l) \rangle \\ & + \Delta U_{\text{rep}}^{\text{QM/MM}} \end{aligned} \quad (2)$$

In this equation  $q_i^A$  is the  $i$ -th point charge of group (molecule) A used

to describe the electrostatic potential of the classical system. The  $Z_j$  are the nuclei in the quantum system. The  $A_{rs}$  are elements of a supermatrix A which describes the response of the total classical polarizable system to the field caused by the quantum system. A can thus be considered as an effective polarizability of the entire classical system.  $V_{sp} = 1/|\mathbf{r}_p - \mathbf{r}_s|$  is the coulomb potential in  $\mathbf{p}$ , brought about by a source in  $\mathbf{s}$ , and  $\mathbf{f}_{sp} = -\nabla_p V_{sp}$  is the corresponding electric field. The scaling factor,  $\gamma$ , is for the dispersion which is discussed below, and  $P_{12}$  is the permutation operator. To distinguish between source and recipient in the expectation values of the field, e.g.,  $\langle f(k;s) \rangle$ , i.e., the electric field at  $\mathbf{s}$  due to electron  $k$ , the electron labels ( $k, l$ ) and the electronic charge ( $e$ ) have been made explicit so as to avoid ambiguity in the signs of the various terms.

In eq 2 the first two terms describe the electrostatic interaction of the nuclei and electrons with the point charges of the solvent. The next two terms describe the interactions between the point charges and the dipoles induced by the nuclei and electrons and vice versa. The fifth and sixth term represent the screening of the nuclear repulsion and attraction, respectively. The seventh and eighth term describe the interaction of an electron with its own and the other electrons' induced dipole moments; the latter term is therefore a two-electron term which contains the induction and part of the dispersion interaction. The scaling factor  $\gamma$  is used for the dispersion and was shown to be roughly equal to the following expression including the second-order perturbation theory expression (SOP) for the dispersion;<sup>29,37</sup>

$$\Delta U_{\text{disp}}^{\text{SOP}} = \left( \frac{E_{\text{solv}}^i}{E_{\text{solv}}^i + E_{\text{solv}}^j} \right) \Delta U_{\text{disp}}^{\text{DRF}} = \gamma \Delta U_{\text{disp}}^{\text{DRF}} \quad (3)$$

where the  $E^i$  are the ionization potentials of the solute and solvent molecules.

The scaling factor  $\gamma$  can be used to redefine the reaction field operator by scaling the integrals for the screening of the one-electron self-energy as well as the two-electron exchange contributions. The latter rescaling is only then possible when the exchange interaction is explicitly defined, i.e., when dealing with a single determinant wave function. The present calculations were therefore performed using  $\gamma = 0$ , and the dispersion interaction was assumed to lead to a uniform lowering of the excitation energy in all solvents.

A full description of the INDO/s-DRF implementation will be published elsewhere.

If the quantum system is omitted in the calculations, the DRF model reduces to a classical force field model in which induction interactions are explicitly accounted for through the presence of polarizabilities.<sup>38</sup> This polarizable force field has been shown to give an excellent description of the many-body terms that arise in systems consisting of multiple polarizabilities.<sup>39</sup> The classical part of the DRF model is typically used to perform molecular dynamics simulations in order to generate solvent configurations around a solute that are later used in the full QM/MM calculations.<sup>30,33</sup>

**Outline of the Simulations.** The experimentally observed influence of a solvent on the absorption or emission spectrum of a solute is in fact an average response over many different solvent configurations. Therefore, it is not sufficient to perform calculations for only one solvent configuration. The QM/MM calculations of the excited states of BA discussed below were averaged over 100 solvent configurations. These configurations were obtained from molecular dynamics (MD) simulations on a fully classical system; i.e., also the BA solute was treated classically. The interactions between the classical molecules (the force field) are expressed in terms of point charges, polarizabilities, and

- (26) Thole, B. T.; Duijnen, P. T. v. *Theor. Chim. Acta* **1980**, *55*, 307–318.  
 (27) Duijnen, P. T. v.; Juffer, A. H.; Dijkman, J. P. *THEOCHEM* **1992**, *260*, 195–205.  
 (28) Vries, A. H. d.; Duijnen, P. T. v.; Juffer, A. H.; Rullmann, J. A. C.; Dijkman, J. P.; Merenga, H.; Thole, B. T. *J. Comput. Chem.* **1995**, *16*, 37–55.  
 (29) de Vries, A. H.; van Duijnen, P. T. *Int. J. Quantum Chem* **1996**, *57*, 1067–1076.  
 (30) Grozema, F. C.; van Duijnen, P. T. *J. Phys. Chem. A* **1998**, *102*, 7984–7989.  
 (31) van Duijnen, P. T.; de Vries, A. H.; Swart, M.; Grozema, F. C. *J. Chem. Phys.* **2002**, *117*, 8442–8453.  
 (32) van Duijnen, P. T.; Swart, M.; Grozema, F. C. *ACS Symp. Ser.* **1999**, *712*, 220–232.  
 (33) Zijlstra, R. W. J.; Grozema, F. C.; Swart, M.; Feringa, B. L.; van Duijnen, P. T. *J. Phys. Chem. A* **2001**, *105*, 3583–3590.  
 (34) Duijnen, P. T. v.; Grozema, F. C.; Swart, M. *THEOCHEM* **1999**, *464*, 191–198.

- (35) Jensen, L.; van Duijnen, P. T.; Snijders, J. G. *J. Chem. Phys.* **2003**, *119*, 12998–13006.  
 (36) Slater, J. C.; Kirkwood, J. G. *Phys. Rev.* **1931**, *37*, 682–697.  
 (37) van Duijnen, P. T. *Int. J. Quantum Chem* **1996**, *60*, 1111–1132.  
 (38) Swart, M.; van Duijnen, P. T. *J. Comp. Chem.* Submitted.  
 (39) Grozema, F. C.; Zijlstra, R. W. J.; van Duijnen, P. T. *Chem. Phys.* **1999**, *246*, 217–227.



repulsion radii on each atom. The point charges for the solvent were derived from *ab initio* Hartree–Fock calculations by fitting them to the electrostatic potential. The atomic polarizabilities were taken from the standard DRF-set<sup>40</sup> that was optimized by fitting them to a set of experimental polarizabilities according to Thole's model for interacting polarizabilities.<sup>41</sup>

In the MD simulations the BA molecule was surrounded by 60 (for cyclohexane, benzene and dioxane) or 100 solvent molecules (for dichloromethane and acetonitrile), representing approximately the first three solvent shells. The solute/solvent systems were confined to a sphere with a radius chosen to approximately reproduce the experimental density of the system. After equilibration for 50 ps, a data-collection simulation of 50 ps was performed. During the data-collection run 100 randomly chosen configurations were saved for use in the full QM/MM simulations. For the BA solute the point charges used in the fully classical MD simulations were taken to be the Mulliken charges for the state of interest.

Singly excited configuration interaction (CI) calculations for the excited states were performed using an INDO/s restricted Hartree–Fock ground state determinant as the reference Hamiltonian. All single excitations from the highest 10 occupied molecular orbitals into the lowest 10 unoccupied molecular orbitals were included in the CI expansion. Further increase in the CI expansion was not found to change the results for the low-lying excited states significantly.

### III. Results and Discussion

**Solvent-Free Bianthryl.** INDO/s configuration interaction calculations of the excited states of bianthryl in its ground state geometry (perpendicular,  $D_{2d}$ ) show that all excited states reflect the symmetry of the molecular framework; only symmetric nondipolar excited states are found. The excitation energy to the LE ( $S_1$ ) state (in a vacuum) was calculated to be 3.47 eV. To gain insight into the nature of the vertical excited states, it is interesting to consider the molecular orbitals and CI configurations involved in the excited states. In the ground state both the highest occupied molecular orbitals (HOMO) and the lowest unoccupied molecular orbital (LUMO) are doubly degenerate. In the case of the HOMOs, one of the degenerate orbitals is almost completely localized on one anthryl unit, while the other is localized mostly on the second anthryl unit (see Figure 2). The same is true for the LUMO levels. Both the HOMO and LUMO orbitals are found to be very similar to the orbitals in the anthracene parent compound. The excitation to the  $S_1$  state is found to be due to a combination of two CI configurations, both involving a local excitation from the HOMO to the LUMO on a single anthryl moiety, in agreement with earlier *ab initio* CI calculations.<sup>18</sup> The  $S_1$  excited state is a bonding combination of these two CI configurations. This immediately explains the similarity between the absorption spectra of anthracene and bianthryl; the absorption spectrum of BA is due to a combination of two locally excited states. The oscillator strength for excitation to the  $S_1$  state is calculated to be 0.59, which is roughly twice as large as the oscillator strength calculated for anthracene. An antibonding combination of the same two CI configurations is also found, at 3.70 eV; however, excitation to this state from the ground state is dipole-forbidden.

At a slightly lower energy, 3.68 eV, two degenerate CI states are found, both consisting mainly of two configurations, one in which an electron is excited from the HOMO on anthryl unit A

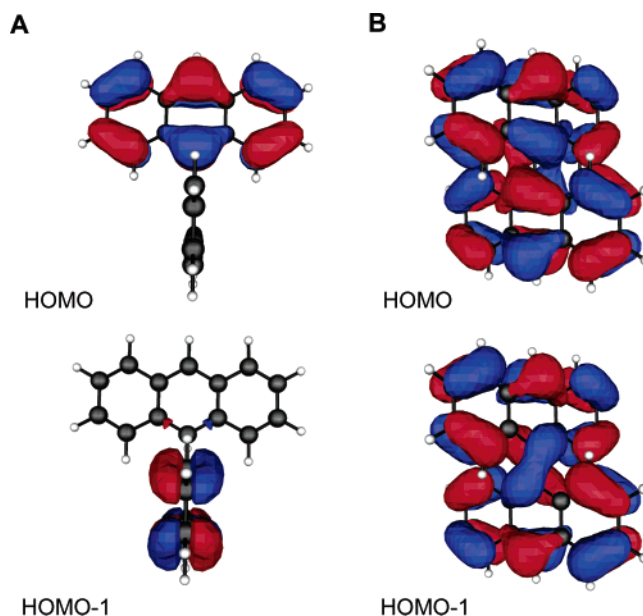


**Figure 2.** Highest occupied molecular orbitals in BA in the perpendicular ground-state geometry (A) and the relaxed excited-state geometry with a dihedral angle of 70° (B).

to the LUMO of anthryl unit B and one in which an electron is excited from the HOMO on B to the LUMO on A. Both of these charge transfer (CT) configurations contribute equally to both of the excited states. Therefore, in absence of symmetry breaking, these states will have no net dipole moment, and hence they should not be called CT states but rather charge resonance (CR) states. Note that the individual CT configurations have large dipole moments of ca. 20 D, close to the value derived from experiments for the CT state in BA. Already a very small deviation from the fully symmetric situation, e.g. an external electric field or asymmetric changes in the bond lengths, is sufficient to lift the degeneracy of the two CR states. This has been demonstrated experimentally by Tanaka et al. who have shown, by using supersonic jet techniques, that complexation with a single acetonitrile molecule is already sufficient to induce charge separation.<sup>42</sup> Symmetry breaking leads to the formation of two charge-separated excited states with opposite dipole moments consisting almost exclusively of a single CT determinant. The energy difference between these two CT-states is then governed by the “strength” of the symmetry breaking. Such a strong effect of symmetry breaking by which the CR states transform into CT states is analogous to occurrence of the so-called “sudden” polarization in twisted ethylene and derivatives.<sup>33,43</sup>

It is generally accepted that, upon excitation to the LE state, the geometry of BA relaxes from the ground-state conformation, in which the anthryl moieties are perpendicular to each other, to a geometry with a twist angle of ca. 70°. <sup>8,9</sup> This geometry relaxation is driven by an increase in the electronic coupling on decreasing the dihedral angle between the anthryl units. In the ground state, the HOMO and HOMO-1, both with the same energy, are doubly occupied. When the mutual angle is decreased from 90°, the degenerate HOMO orbitals start interacting, leading to a pair of new HOMOs, a bonding and an antibonding combination of the HOMO orbitals in the

(40) van Duijnen, P. T.; Swart, M. *J. Phys. Chem. A* **1998**, *102*, 2399–2407.

(41) Thole, B. T. *Chem. Phys.* **1981**, *59*, 341–350.

(42) Tanaka, K.; Honma, K. *J. Phys. Chem. A* **2002**, *106*, 1926–1932.

(43) Mulliken, R. S. *Phys. Rev.* **1932**, *41*, 751–758.

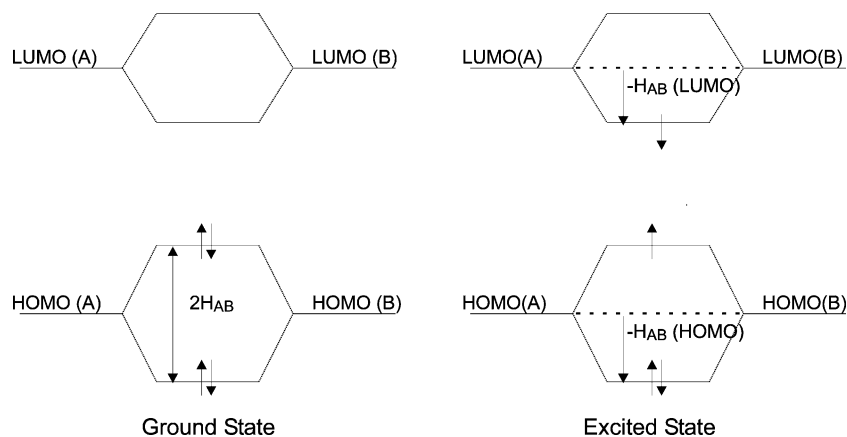


**Figure 3.** Energy level diagram for BA ground and excited state.

perpendicular geometry (Figure 2). The energy splitting between these two new orbitals is, in a simplified two-state model, equal to 2 times the electronic coupling,  $H_{AB}$ , between the original HOMOs on the anthryl units; see Figure 3. The same is true for the LUMO orbitals. In the electronic ground state, where both of these new levels are doubly occupied, this does not lead to a lower energy since one of the new levels is lower than the original HOMO by  $H_{AB}$  and the other is higher by almost the same amount. Therefore, the dihedral angle between the units is dictated by steric interactions, forcing BA to be perpendicular in the ground state. In the ( $S_1$ ) excited-state one electron is excited from the HOMO orbital to the LUMO as indicated in Figure 3. In this case deviations from a perpendicular geometry do lead to a lower energy. The energy of the electron in the LUMO is lowered by  $H_{AB}(\text{LUMO})$  and the doubly occupied HOMO-1 level decreases in energy by  $H_{AB}(\text{HOMO})$ , whereas the singly occupied level goes up by the same amount. This energy lowering is counteracted by an increase in steric repulsion upon deviation from a perpendicular geometry leading to an intermediate angle of ca.  $70^\circ$  where the energy is minimal. The differences between the torsional potentials in the ground and excited state have been studied theoretically for 9-phenyl-anthracene. The ground state was shown to exhibit a rather flat potential energy surface of ca.  $90^\circ$ , while the  $S_1$  state shows two minima ca.  $60^\circ$  and  $120^\circ$ .<sup>44</sup>

The relaxation to an angle of  $70^\circ$  leads to a considerable Stokes shift in the emission from the LE state. The calculated transition energy at an angle of  $70^\circ$  was 3.38 eV, almost 0.1 eV lower than that for the perpendicular geometry. The oscillator strength is similar, 0.50. The excited state at an angle of  $70^\circ$  is dominated by only one CI configuration in which an electron is excited from the HOMO (at an angle of  $70^\circ$ , which is now equally distributed over both anthryl units) to the LUMO (also fully delocalized).

The description of the excited states of BA at  $90^\circ$  and at  $70^\circ$  was based on different orbitals for the ground state; i.e., the reference determinant was different (see Figure 2). However, the total wave function of the lowest excited state is very similar in both cases, the only difference being the increased coupling at nonperpendicular angles.

The increased electronic coupling upon lowering the interunit angle from  $90^\circ$  is expected to result in a considerable increase in the excited state polarizability. From experimental studies,

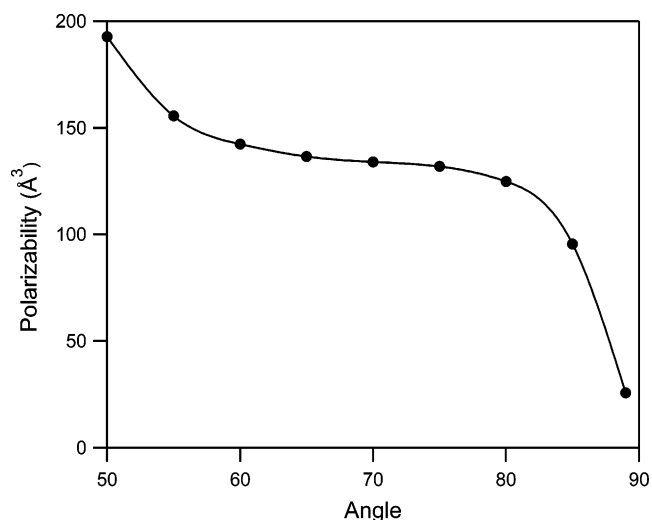


**Figure 4.** Excess polarizability for the  $S_1$  state in bianthryl as a function of the twist angle.

usually the increase in polarizability upon excitation or excess polarizability is obtained, rather than the excited-state polarizability itself. Therefore, in the following, the polarizabilities reported are excess polarizabilities,  $\Delta\alpha$ . The increase in polarizability was studied by repeating the INDO/s-CIS calculations but now including an external electric field along the bond connecting both anthryl units. Application of an electric field along the other axes was found to give negligible contributions to the overall polarizability; therefore, the average excess polarizability,  $\Delta\bar{\alpha}$ , is equal to one-third of the polarizability component along the bond between the anthryl units. The excess polarizability of the  $S_1$  excited state is shown in Figure 4 as a function of the dihedral angle in the static electric field. The polarizability is very small at  $90^\circ$ , corresponding to an excess polarizability,  $\Delta\bar{\alpha}$ , of ca.  $10 \text{ \AA}^3$ . The excess polarizability rapidly increases when the dihedral angle decreases, reaching a plateau of ca.  $70^\circ$ . The excess polarizability at  $70^\circ$  is ca.  $130 \text{ \AA}^3$ . If the angle is decreased below  $60^\circ$ , the induced dipole moment, and thus the excess polarizability increases more rapidly again.

The calculated values for  $\Delta\bar{\alpha}$ , discussed here can be compared directly to experimentally measured excess polarizabilities. For the vertical transition to the Franck–Condon state an excess polarizability of  $17 \text{ \AA}^3$  has been found in electro-absorption measurements.<sup>45</sup> This value is close to the calculated value for  $\Delta\bar{\alpha}$  at a dihedral angle of  $90^\circ$ . For the relaxed  $S_1$  state  $\Delta\bar{\alpha}$  was

(44) Sakata, K.; Hara, K. *Chem. Phys. Lett.* **2003**, 371, 164–171.

**Table 1.** Solvent Polarity Parameter, Local Electric Field ( $F$ ), Field Relaxation Times ( $t_{1/2}$ ), and Induced Dipole Moment for BA with a Twist Angle of  $70^\circ$ <sup>a</sup>

solvent	$E_T(30)$	electric field (au)	$t_{1/2}$ (ps)	induced dipole (D)
cyclohexane	30.9	$6.44 \times 10^{-4}$	15.9	0.74
benzene	34.3	$2.78 \times 10^{-3}$	3.9	5.32
dioxane	36.0	$4.87 \times 10^{-3}$	18.1	5.72
dichloromethane	40.7	$3.01 \times 10^{-3}$	0.2	7.03
acetonitrile	45.6	$4.24 \times 10^{-3}$	0.4	8.54

<sup>a</sup> The solvent shell is equilibrated using *symmetric* charge distribution for bianthryl.

measured by two techniques; a value of  $200 \text{ \AA}^3$  was found in flash-photolysis time-resolved microwave conductivity measurements,<sup>12</sup> while a value of  $220 \text{ \AA}^3$  was derived from electro-emission experiments by Baumann et al.<sup>6,13</sup> Although the calculated  $\Delta\alpha$  is somewhat lower than both experimental values, the large increase in polarizability upon transition from the vertical excited to the relaxed  $S_1$  state is reproduced. The underestimation of  $\Delta\alpha$  by the calculations is likely to be caused by the basis set used in the INDO/s calculations. A minimal basis set was used, as is usual in semiempirical calculations; however, for accurate polarizability calculations it is generally necessary to use large basis sets. These calculations confirm that the formation of a relaxed  $S_1$  state in BA exhibiting a decreased interunit angle is indeed accompanied by a large increase in polarizability of the excited state.

**Formation of a Dipolar Relaxed Excited State in BA.** Now that it has been established that the torsional relaxation around the central  $\sigma$ -bond leads to a large increase in the polarizability, it is of interest to consider whether a solvent shell around BA can induce a dipole moment in the  $S_1$  state. In time-resolved microwave conductivity experiments (TRMC) it was shown that even in weakly polar solvents the relaxed  $S_1$  state exhibits a considerable dipolar nature.<sup>10–12</sup> Dipole moments of ca. 7 D were measured in benzene and dioxane, which is considerably smaller than the value of 20 D obtained for the CT state from optical measurements and from TRMC measurements on cyano-substituted BA. Although both benzene and dioxane possess no permanent dipole moment, they still exhibit some polar nature because of their quadrupole moment (or local bond dipoles).

To study the “local” electric field in different solvents, a molecular dynamics simulation was performed in which a polarizable probe sphere with a radius of  $3.7 \text{ \AA}$  was surrounded by 100 (for dichloromethane and acetonitrile) or 60 (benzene, dioxane, and cyclohexane) solvent molecules. The dipole moment induced by the solvent in the probe sphere was saved every 100 fs during an MD simulation of 500 ps. The root-mean-square values for the local electric field in the solvent are given in Table 1. It is clear that although the average local field in the solvent is negligible, the fields can be very high at a specific moment in time; even in a nonpolar solvent such as cyclohexane, the root-mean-square local electric field was calculated to be  $6.44 \times 10^{-4}$  atomic units ( $1 \text{ au} = 5.14 \times 10^{11} \text{ V/m}$ ). In the weakly polar solvents benzene and dioxane the local electric fields are significantly higher,  $2.78 \times 10^{-3} \text{ au}$  and  $4.87 \times 10^{-3} \text{ au}$ , respectively. It is also interesting that in the polar solvents dichloromethane and acetonitrile the local electric field is similar to that in the weakly polar solvents.

It should be noted that the local electric field as monitored above by a probe-sphere with a point-polarizability cannot be used directly with e.g. the average (point) polarizability of a bianthryl molecule to calculate the induced dipole moment since the actual molecule feels the surrounding solvent as a distributed set of charges. To calculate the solvent-induced dipole moment in BA with a dihedral angle of  $70^\circ$ , a fully classical MD simulation, in which BA was present, was performed during which 100 randomly chosen solvent configurations were saved. In these MD simulations the charge distribution on the BA molecule is completely symmetric, the gas-phase charge distribution for the relaxed  $S_1$  state. Therefore, if any dipole formation is observed, it is due to the inherent local electric field in the solvent.

For the 100 saved configurations a mixed quantum mechanical/molecular mechanical simulation was performed. The solvent is described by classical mechanics, while the solute, BA, is described by a CIS wave function using the RHF INDO/s reference Hamiltonian. This calculation yields the wave function and the excitation energy for the lowest 10 excited states in the presence of the solvent. The magnitudes of the dipole moment of BA in the relaxed  $S_1$  state, averaged over the 100 saved configurations, are listed in Table 1. For benzene and dioxane, excited dipole moments of 5–6 D were obtained. This shows that these weakly polar solvents can induce considerable dipole moments in the highly polarizable relaxed excited state of BA. This is in agreement with time-resolved microwave conductivity experiments in which dipole moments of 6.9 and 7.5 D were measured for benzene and dioxane, respectively.<sup>12</sup> The calculated dipole moments are somewhat lower than the experimental values which may be caused by the use of a limited basis set in the quantum chemical calculations as mentioned above. The induced dipole moment obtained in cyclohexane is rather small, much smaller than that observed experimentally.

In more polar solvents the induced dipole moments are even higher, 7.03 and 8.54 D for dichloromethane and acetonitrile, respectively. It appears that the  $S_1$  dipole moment increases with the solvent polarity expressed in terms of the  $E_T(30)$  scale.<sup>46</sup>

Now that it has been confirmed theoretically that considerable dipole moments can be induced in the excited state of bianthryl, even in weakly polar solvents, it is of interest to consider the time scale for dipole relaxation in these solvents. The microwave conductivity measurements give information not only on the magnitude of the dipole moments in different solvents but also on the time scale for dipole relaxation (i.e., randomization of the net dipole moment). From these TRMC experiments the dipole relaxation time was determined to be of the same order of magnitude as the reciprocal radian frequency of the microwaves used, corresponding to ca. 15 ps for 10 GHz microwaves.<sup>12</sup> This is much shorter than the relaxation time expected if the dipole relaxes by rotational diffusion involving rotation of the whole bianthryl molecule, which was estimated to be 100–300 ps depending on the solvent viscosity.<sup>12</sup> Dipole relaxation times on this order of magnitude were in fact found for cyano-substituted BA where the intramolecular symmetry breaking is expected to lead to a CT state, even in nonpolar solvents.<sup>12</sup> This led to the conclusion that dipole relaxation mainly takes place via a so-called flip-flop mechanism in which

(45) Liptay, W.; Walz, G.; Baumann, W.; Schlosser, H.-J.; Deckers, H.; Detzer, N. *Z. Naturforsch.* **1971**, *26a*, 2020–2038.

(46) Reichardt, C. *Chem. Rev.* **1994**, *94*, 2319–2358.



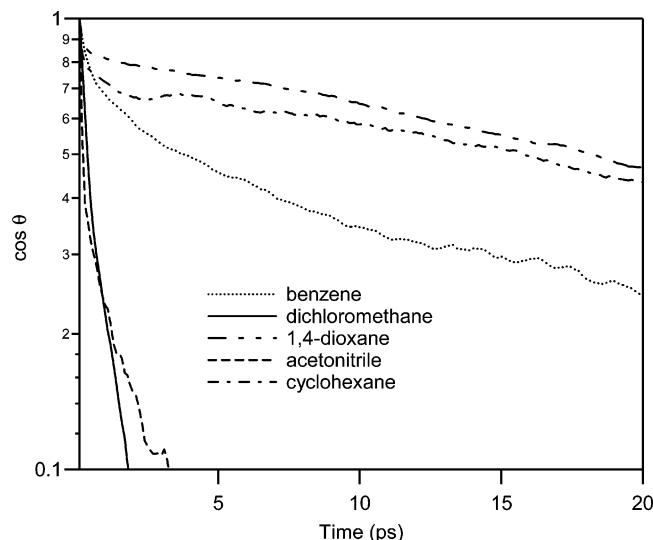


**Figure 5.** Relaxation of the direction of the local electric field in benzene, dichloromethane, acetonitrile, 1,4-dioxane, and cyclohexane.

the direction of the dipole moment changes without changes in the nuclear positions.

In connection with these microwave experiments, calculations have been performed in order to estimate the relaxation time of the induced dipole moment in the relaxed  $S_1$  state in BA in different solvents. The relaxation times of the electric field were calculated from the solvent configurations saved in the MD simulations with the probe sphere. The calculated decay of the direction of the electric field,  $\vec{E}$ , expressed as the cosine of the angle between  $\vec{E}(t=0)$  and  $\vec{E}(t)$ , in time is shown in Figure 5, and the half-life times are listed in Table 1. For all of the solvents considered the decay is nonexponential as evident from the nonlinear curves in the semilogarithmic plot in the figure. This means that the decay rate is not constant in time. This nonexponential decay is analogous to the nonexponential dielectric relaxation of solvents. Such nonexponential or non-Debye relaxation has been generally observed, and several theories have been developed to explain such behavior.<sup>47,48</sup> In these theories the non-Debye relaxation is either due to an ensemble of noninteracting dipoles that have a different local environment or due to interaction between solvent dipoles.

For the polar solvents dichloromethane and acetonitrile the dipole relaxation time is very short, less than a picosecond. The relaxation time of the electric field can be related to the rotational relaxation time of the solvent used, although it should be noted that there is no direct relation between the two since the field is due to the collective effect of many solvent molecules. For acetonitrile the “tumbling” diffusion time (rotation of the long axis of the molecule) was measured to be ca. 10 ps in the pure solvent, whereas for the rotation around the long axis a diffusion time of less than a picosecond was found.<sup>49</sup> From optical Kerr effect measurements solvent relaxation times of the order of a picosecond have been reported for acetonitrile at room temperature which is of the same order of magnitude as the field decay time of 0.4 ps found from the simulations performed here.<sup>50,51</sup> The calculated field relaxation

time for dichloromethane is a factor of 2 shorter than that for acetonitrile which can be explained by the more compact structure of the molecule and hence a smaller rotational diffusion time.

For the weakly polar solvents benzene and dioxane, the field relaxation times are an order of magnitude larger than those for dichloromethane and acetonitrile as evident from Figure 5. For benzene a field-half-life time of 3.9 ps was calculated which is comparable to the relaxation time value 7.9 ps from microwave experiments. Rotational relaxation times of the order of 10 ps (for rotation around the  $C_6$  axis) and 20 ps (for rotation perpendicular to the  $C_6$  axis) have been reported experimentally,<sup>52</sup> which is on the same order of magnitude as the field relaxation times found here. Optical Kerr effect measurements on benzene also give relaxation times of ca. 3 ps which agrees with the field relaxation time reported here.<sup>51,53</sup> In dioxane, the field relaxation time was calculated to be significantly longer; a half-life time of 18.1 ps was found, whereas experimental data give a relaxation time of 14 ps in this case. The considerably longer decay time for the field in dioxane as compared to benzene can be understood in terms of the larger solvent viscosity ( $\eta = 0.65$  cP for benzene and  $\eta = 1.41$  cP for dioxane) which will lead to longer rotational diffusion times.

For cyclohexane the relaxation half-life time is comparable to that calculated for dioxane, 15.9 ps. This is much longer than the dipole relaxation time obtained from TRMC experiments (2 ps). However, it should be noted that the decay of the electric field direction is rather nonexponential, especially in the case of cyclohexane. At a time scale of a few tenths of a picosecond the decay is very fast, significantly faster than those for dioxane and benzene. After 0.5 ps the curves for cyclohexane and benzene cross and the decay rate decreases. This large change of the decay rate with time makes it difficult to compare calculated and experimental data for cyclohexane. The large difference between the experimentally found dipole relaxation times in cyclohexane and benzene are not reflected in the rotational diffusion times. The rotational diffusion times for cyclohexane ( $\sim 10$  ps)<sup>54</sup> are of the same order of magnitude as that for benzene.

From the comparison of the calculated field relaxation times in benzene and dioxane with the dipole relaxation times for the relaxed  $S_1$  state in BA, it is concluded that the rapid flip-flop dipole reversal is likely to be due to reorientation of the molecules in the first solvent shell, leading to a change in the direction of the induced dipole moment in BA.

**Solvatochromism.** The absorption spectrum of BA is virtually solvent-independent. The emission spectrum exhibits rather strong solvatochromism in polar solvents, whereas the solvent effect is much smaller for apolar solvents. The nature of the excited state that is responsible for the emission is not the same for all solvents. In apolar and weakly polar solvents the relaxed  $S_1$  state is held to be responsible for the emission. In polar solvents fluorescence is due to a highly dipolar excited state, the CT state. QM/MM simulations have been performed in order

(47) Magee, M. D. *J. Chem. Soc., Faraday Trans. 2* **1974**, 70, 929–938.

(48) Hill, R. M.; Dissado, L. A. *J. Phys. C: Solid State Phys.* **1985**, 18, 3829–3836.

(49) Wakai, C.; Saito, H.; Matubayasi, N.; Nakahara, M. *J. Chem. Phys.* **2000**, 112, 1462–1473.

(50) Foggi, P.; Bartolini, P.; Bellini, M.; Giorgini, M. G.; Morresi, A.; Sassi, P.; Cataliotti, R. S. *Eur. Phys. J. D* **2002**, 21, 143–151.

(51) Loughnane, B. J.; Scodinu, A.; Farrer, R. A.; Fourkas, J. T.; Mohanty, U. *J. Chem. Phys.* **1999**, 111, 2686–2694.

(52) Witt, R.; Sturz, L.; Dolle, A.; Muller-Plathe, F. *J. Phys. Chem. A* **2000**, 104, 5716–5725.

(53) Ratasjka-Gadomska, B. *J. Chem. Phys.* **2002**, 116, 4563–4576.

(54) Tanabe, K. *Chem. Phys. Lett.* **1981**, 83, 397–400.

**Table 2.** Calculated Absorption Energies and Emission Energies for the Relaxed Excited  $S_1$  State and the CT State of Bianthryl in Different Solvents

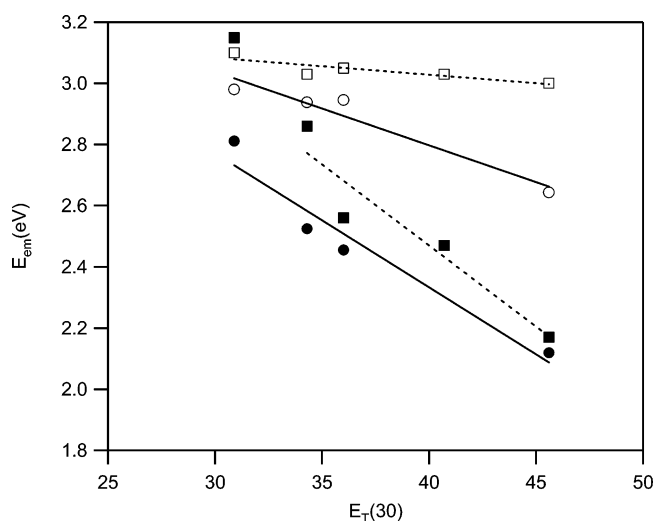
solvent	$E_T(30)$	$E_{abs}$ in eV	$E_{em}(S_1, 70^\circ)$ in eV	$E_{em}(CT, 90^\circ)$ in eV
cyclohexane	30.9	3.14	3.10	3.15
benzene	34.3	3.07	3.03	2.86
dioxane	36.0	3.07	3.05	2.56
dichloromethane	40.7	3.19	3.03	2.47
acetonitrile	45.6	3.19	3.00	2.17

to examine the solvent effect on the emission from the relaxed  $S_1$  state and the CT state. For this purpose the quantum mechanically described solute (BA) was surrounded by a solvent shell containing either 60 or 100 solvent molecules, as discussed in section II. Full QM/MM calculations were performed for 100 randomly chosen solvent configurations obtained from the fully classical MD simulation.

The solvent effect on the electronic absorption spectrum can be divided into different contributions, the electrostatic part, the induction part, and the dispersion part.<sup>30</sup> The electrostatic interactions between the solute and solvent in the ground and excited state will be different in different solvents. This causes a shift in the absorption spectrum, either to higher energy or to lower energy. Strong solvent shifts due to the electrostatic contribution are found only when the charge distribution in the solute is very different for the ground state and the excited state. The polarization contribution is related to different induction interactions (dipole–induced dipole) between the solute and solvent in the ground and excited state. Finally, the dispersion contribution is related to the change in polarizability of the solute upon excitation, which is positive in general. This contribution leads to a lowering of the excitation energy. In this work dispersion was assumed to lead to a uniform lowering of the excitation energies by  $\sim 0.3$  eV. This value is based on preliminary calculations where the dispersion was included.

First of all, the solvent effect on the absorption spectrum was considered. In this case the solvent configurations were obtained by taking the interunit dihedral angle between the two anthryl units equal to  $90^\circ$ . The point charges on BA were taken to be the Mulliken charges obtained from an INDO/s calculation for the ground state. The calculated absorption energies for BA in the five solvents considered in this work are listed in Table 2. The absorption energy is relatively insensitive to the solvent; all excitation energies are between 3.1 and 3.2 eV. These values are in good agreement with experimental absorption maxima which are ca. 3.2 eV for all solvents. The values listed in Table 2 correspond to the allowed transition in perpendicular BA where, in all cases, the excited state has a small dipole moment. This transition is not the lowest transition in all solvent configurations.

If the excited states are examined, it is found that in all solvents the fully symmetric (vacuum) CR states (combinations of two CT determinants) have been replaced by two CT states. This is even the case in cyclohexane which shows that an asymmetric distribution of polarizabilities (i.e., local density fluctuations) causes enough symmetry breaking to lead to fully charged separated states in the perpendicular geometry. These CT states are close in energy, or often even lower than, the dipole-allowed vertical excited state, even in cyclohexane. This behavior is analogous to the occurrence of sudden polarization

**Figure 6.** Experimental (full lines) fluorescence energies for bianthryl (open circles) and cyano-bianthryl (closed circles) and calculated (dotted lines) fluorescence energies for the relaxed  $S_1$  state (open squares) and the CT state (closed squares) of BA as a function of the  $E_T(30)$  solvent polarity parameter.

in twisted ethylene.<sup>33,43</sup> If the angle between the anthryl units is lowered, the CT states disappear because of increased coupling between the units. In this strongly coupled BA, the excited states tend to be delocalized over the entire BA molecule and a much stronger symmetry breaking is needed to induce an appreciable dipole moment, as discussed above.

The emission from the relaxed  $S_1$  state was studied by considering a BA solute molecule with a fixed dihedral angle of  $70^\circ$ . The solvent configurations were obtained from classical MD simulations with a symmetric charge distribution on the BA molecule (the vacuum Mulliken charges). The 100 saved conformations for which a QM/MM calculation of the spectrum was performed are the same as those used in the calculation of the induced dipole moment discussed above. The calculated emission energies for the relaxed  $S_1$  state are listed in Table 2. The emission from the relaxed  $S_1$  state is found to be almost independent of the solvent, which is in agreement with a lack of solvent dependence in the emission energy found experimentally in weakly polar solvents. Comparison with experimental data in nonpolar and weakly polar solvents shows that the calculated emission energies are in good agreement with measured spectra; both the calculated and experimental values are ca. 3 eV. The small dependence of the emission energy on the solvent polarity shown in Figure 6 indicates that the difference between the electrostatic interactions between solute and solvent in the ground and excited state is rather small. Comparison of the calculated solvent dependence to the experimental slope for BA, also shown in Figure 6, shows that up to an  $E_T(30)$  solvent polarity<sup>46</sup> of 36 (dioxane) the trend is very similar. For higher solvent polarities the emission energy decreases much faster in the experimental data than in the calculated values. This is understood by the fact that in polar solvents such as acetonitrile ( $E_T(30) = 45.6$ ) the emission is dominated by the charge transfer state, and not due to the relaxed  $S_1$  state that is explicitly considered here.

To study the fluorescence from the charge transfer state, classical MD simulations were performed in which the BA solute (with a dihedral angle of  $90^\circ$ ) was dressed with point charges that correspond to the CT state. These point charges



were obtained from a Mulliken population analysis of a single determinant where an electron is transferred from one anthryl moiety to the other. This charge distribution leads to a solute with a dipole moment close to 20 D, the value expected for the fully charge-separated excited state. In this way the solvent is allowed to fully relax to the CT state in BA, and the QM/MM CIS calculations on the saved configurations refer explicitly to emission from the CT state. This was confirmed by examining the dipole moment of the lowest excited state averaged over the saved solvent configurations, which was found to be close to 20 D in all cases. The calculated emission energies are listed in Table 2 and are also shown in Figure 6 as a function of the solvent polarity. The large excited state dipole moment leads to a strong effect of solvent polarity on the emission energy as evident from Figure 6. The calculated emission energy decreases from 3.14 eV in cyclohexane to 2.15 eV in acetonitrile, a shift of almost 1 eV. The strong solvent shift is mostly due to the electrostatic component; dispersion again leads to a uniform lowering of the emission energy for all solvents. From comparison with the experimental data for the emission from BA it appears that the calculations considerably underestimate the emission energies. It is more interesting to compare the slope of the solvent dependence to the experimental data. The calculated slope is somewhat larger than that measured for BA. Comparing the slopes is troubled by the fact that in the experimental data for BA the emission at low solvent polarity is actually from the relaxed  $S_1$  state and not from the CT state. Therefore the emission energies for cyano-substituted BA are also shown in Figure 6. In cyano-substituted BA (CBA), the symmetry is broken by substituting one of the anthryl units with an electron withdrawing group. This leads to an intramolecular stabilization of the CT state. Therefore in the case of CBA the emission is expected to be always from the CT state. The slope of the solvent dependence for CBA is very similar to that found from the calculations for the fully charge-separated state in BA. This leads to the conclusion that in BA, even in polar solvents, the emission is not completely due to the charge-separated state. In the calculations discussed here, two well-defined states were created, a relaxed  $S_1$  state with a fixed interunit angle of  $70^\circ$  and a CT state with a twist angle of exactly  $90^\circ$ . In reality the emission is likely to be due to a distribution of different molecular conformations, some with dihedral angles a ca.  $70^\circ$  giving rise to relaxed  $S_1$  state-like emission, and others with dihedral angle close to  $90^\circ$  causing CT-like emission.

#### IV. General Discussion and Summary

The results obtained from the calculations presented above give valuable insight into the role of the solvent in the formation of the charge-separated excited state in BA. First of all, excitation initially leads to the formation of a "locally excited state" which consists of a linear combination of two CI determinants, both corresponding to local HOMO–LUMO excitations on the individual anthryl moieties. The absorption energy is almost independent of the solvent polarity which supports the nonpolar nature of the locally excited state. At somewhat higher energy two charge-resonant (CR) states are present that consist of symmetric combinations of two CT determinants. In the presence of an asymmetric environment the CR states transform into two CT states. It should be noted that these CT states are mixtures of multiple determinants. However, in the presence of symmetry breaking they are

dominated by a single CT determinant; i.e., they are effectively a CT state. It was found that an asymmetric distribution of polarizabilities (i.e., local density fluctuations) is sufficient to induce the symmetry breaking of the electronic structure in the (close-to) perpendicular geometry. These CT states are close in energy to the initially excited, local excited state. The energetic proximity of the LE and CT states supports the recent suggestion by Kovalenko et al.<sup>55</sup> that upon excitation of BA a quasi-stationary distribution of LE and CT states is obtained already on a very short time scale ( $<10$  fs). The population dynamics of the CT and LE states occurs on a longer time scale, since it is closely coupled to the solvation time. In polar solvents the distribution shifts toward the CT state since this state is stabilized by electrostatic interactions with the solvent. This leads to an increase in CT population on the time scale of tens of picoseconds.<sup>15,56–58</sup>

In apolar solvents the solvent cannot sufficiently stabilize the CT state to drive the population toward the fully charge-separated state. Instead, intramolecular relaxation leads to the formation of an excitonic state, the relaxed  $S_1$  state. In the relaxed  $S_1$  state the interunit angle decreases since an increased coupling between the units leads to a lowering of the total electronic energy. This lowering is counteracted by an increase in the steric interactions between the subunits, and a balance is found at an angle close to  $70^\circ$ , the geometry of the relaxed  $S_1$  state.<sup>4,8,9,44,59</sup> Upon decreasing the interunit angle from  $90^\circ$  to  $70^\circ$  the polarizability of the relaxed  $S_1$  state of BA increases by an order of magnitude, in agreement with excess polarizability data from time-resolved microwave conductivity (TRMC) measurements<sup>12</sup> and electroabsorption/emission experiments.<sup>45</sup> In the case of an asymmetric solvent shell there is always a net electric field in the solvent at the site of the BA solvent. This local solvent electric field can induce a considerable dipole moment in the relaxed  $S_1$  state, as was shown by QM/MM calculations. This is in agreement with TRMC experiments in which it was shown that BA exhibits a considerable excited state dipole moment of ca. 7 D in weakly polar and apolar solvents.<sup>12</sup> This dipole moment is still much smaller than the dipole moment expected for the CT state (20 D). These calculations show that the dipole moment observed in weakly polar and nonpolar solvents can be explained in terms of the relaxed  $S_1$  state with a considerable induced dipole moment without the need to assume a thermal equilibrium between the CT state and the relaxed  $S_1$  state.<sup>4,5,14,15,56</sup> This conclusion is supported by the absence of absorption features characteristic of radical anions and cations of anthracene in weakly polar solvents; features which are, however, observed in polar solvents such as acetonitrile and butyronitrile.<sup>5,6,17</sup>

The dipole moment induced by the solvent changes direction with motion of the solvent molecules around BA. The time scale on which the direction of the induced dipole moment decays depends on the nature of the solvent but is on the same order of magnitude as the rotational solvent relaxation times for the

- (55) Kovalenko, S. A.; Perez-Lustres, J. L.; Ernstring, N. P.; Rettig, W. *J. Phys. Chem. A* **2003**, *107*, 10228–10232.
- (56) Kang, T.-J.; Jarzeka, W.; Barbara, P. F.; Fonseca, T. *Chem. Phys.* **1990**, *149*, 81–95.
- (57) Jurczok, M.; Plaza, P.; Rettig, W.; Martin, M. M. *Chem. Phys.* **2000**, *256*, 137–148.
- (58) Nagarajan, V.; Brearley, A. M.; Kang, T.-J.; Barbara, P. F. *J. Chem. Phys.* **1987**, *86*, 3183–3196.
- (59) Elich, K.; Kitazawa, M.; Okada, T.; Wortmann, R. *J. Phys. Chem. A* **1997**, *101*, 2010–2015.

pure solvents. The calculated decay times are ranging from a few picoseconds for the small-molecule solvents dichloromethane and acetonitrile and of the order of 10–20 ps for cyclohexane, benzene, and dioxane. The latter dipole relaxation times are similar to the values obtained from TRMC measurements, 8 ps for benzene and 14 ps for dioxane. Both values are much smaller than the dipole relaxation time expected when the relaxation involves rotation of the whole BA molecule (200–300 ps) which leads to the conclusion that the dipole relaxation observed in the measurements is actually due to reorientations in the solvent shell, which leads to relaxation of the *induced* dipole moment. Note that in this case the fluctuations in the solvent shell are the source of the dipole relaxation; i.e., the induced dipole moment changes direction. This is different from the solvent reorganization encountered in electron transfer reactions where the formation of a highly dipolar state induces solvent reorganization. In the latter case the size and direction (and relaxation) of the excited-state dipole moment do not depend on the nature and relaxation dynamics of the solvent, while in the present case the solvent is the source of the dipole moment and also determines the dipole relaxation time.

The experimental slope of the solvent dependence of the fluorescence maximum of bianthryl is smaller than that calculated for the fully charge-separated state; however, it is still considerably larger than that calculated for the relaxed  $S_1$  state.

This indicates that a distribution of excited-state geometries, with a twist angle ranging from 70° to 90°, is responsible for the fluorescence. The average excited state dipole moment, and therefore also the emission energy, depends strongly on the twist angle. The emission that is measured is caused by the full ensemble of excited conformations together. In apolar and weakly polar solvent the fluorescence is almost exclusively due to fluorescence from the relaxed  $S_1$  state. In more polar solvents the fluorescence originates mainly from the CT state; however, it should be noted that even in acetonitrile a small but readily observable shoulder in the fluorescence spectrum exhibiting emission from the relaxed  $S_1$  state has been reported.<sup>12</sup>

**Supporting Information Available:** Tables S1 and S2 contain the atomic coordinates for 9,9'-bianthryl in the perpendicular and 70° conformation. The partial charges and repulsion radii on all atoms used to calculate the electrostatic interactions in the classical and QM/MM calculations are also listed. For the perpendicular geometry two sets of charges are given; for the locally excited state (LE) and for the CT state. Tables S3–S7 contain coordinates, partial charges, and repulsion radii for the solvents used. The coordinates and radii are given in atomic unites (bohr). This material is available free of charge via the Internet at <http://pubs.acs.org>.

JA051729G